AERODYNAMICS ANALYSIS OF A FORMULA SAE CAR

Sahil Gupta* and Kishal Saxena
*Author for correspondence
Department of Aerospace Engineering and Department of Engineering Design,
Indian Institute of Technology Madras,
Chennai, 600036,
India,
E-mail: ae13b046@smail.iitm.ac.in

ABSTRACT

Formula SAE is a college-level student design competition where every year students of universities all over the world build and compete with an open-wheel formula-style race car. A Formula SAE car spends more time on corners than on straight line track and hence, the aerodynamic loads play a significant role while concerning, helping in reducing the overall lap timings of the race car. In this study, the main goal is design and CFD analysis of the aerodynamics package of the race car which includes a front wing, a rear wing and an under tray. Society of Automotive Engineers (SAE) focuses on developing a simple, lightweight, easily operated open chassis vehicle for this competition. Compliance with SAE rules is compulsory and governs a significant portion of the objectives. This aerodynamics study of a race car is focused towards reducing drag and at the same time optimizing the down force generated to achieve minimized lap timings.

INTRODUCTION

Formula SAE challenges the students to build a formula-style race car. Since the inception of the competition, the design has been continuously evolving and changing. One development that seems to very common these days is about producing downforce in the FSAE car using various aerodynamic components. In this paper, design and analysis of aerodynamics package of Raftar Formula Racing (FSAE team of IIT Madras) are presented. In order to achieve better performance, the vehicle has to be aerodynamically efficient. The drag force is unwanted, which normally acts against the driving force of the car, while downforce is useful in maintaining the race car on the ground. The aerodynamic forces enable the car to move faster in corners and improve performance tremendously.

The organization of this paper is as follows. Calculations of design values are presented, based on lap timing simulation software: OptimumLap [14]. In subsequent sections, flow simulations of components and full body, benchmark studies, and an optimization study performed using ANSYS are discussed. The design values were established before design and simulations were performed.

As the primary objective of the competition is optimization of lap timings, an optimum value for drag and downforce coefficients were found using maximum power calculations and simulations in Optimum Lap (lap timings simulation software by OptimumG) [14].

NOMENCLATURE

L	[kgm/sec^2]	Downforce (negative of lift force)
D	[kgm/sec^2]	Drag force
A	[m^2]	Frontal area of body
ρ	[kg/m^3]	Density of Air
c_L	[-]	Downforce coefficient
c_D	[-]	Drag coefficient
P	[kgm^2/sec^3]	Power of engine
p	[kg/msec^2]	Pressure

Subscripts

RW	Rear wing
FW	Front wing

A detailed flowchart of various steps involved in design value estimation is presented in Figure 1.

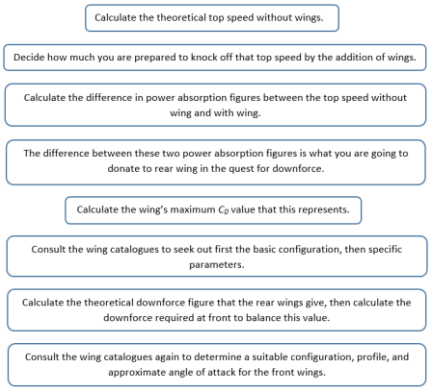

Figure 1 Design values flowchart

KTM 390cc engine was used on the car; after rig testing, the maximum power available was estimated to be around 17.2 kW. On a Formula Student race track, maximum allowable speed is around 110 km/hr [6] and corresponding power requirement was calculated (1) to be 9.3 kW.

$$P_{req} = \frac{1}{2}\rho v^3 A c_D \quad (1)$$

The remaining power available was 7.9 kW. This power can be donated for overcoming the increased drag due to the addition of aerodynamic components on the car. The problem was now reduced to finding an optimum value for drag, such as to obtain minimum lap timings. This was carried out using simulations in Optimum Lap and correlating it with experimental data from Mcbeath [10]. The experimental data relates drag and

downforce coefficient for rear wings, commonly used in the motorsport industry. From (1),

$$A_{RW} C_{D\,RW} = 1.106\ m^2$$

Furthermore, SAE rulebook for Formula Student [12] restricts the maximum allowable area for rear wing to 0.72 m^2. Hence, the maximum achievable value for drag coefficient was 1.6. The interference drag due to rear wing has been ignored for these calculations.

A batch run simulation was performed in Optimum Lap and these data points were correlated with experimental data. From the filtered data points, minimum lap timing corresponded to value of 1.53 for drag coefficient and 3.6 for downforce coefficient. As this value of drag coefficient was below maximum achievable value, it was acceptable. Using these initial estimates of force coefficients, design values for front wing were obtained using moment balance about the center of gravity (Fig. 2).

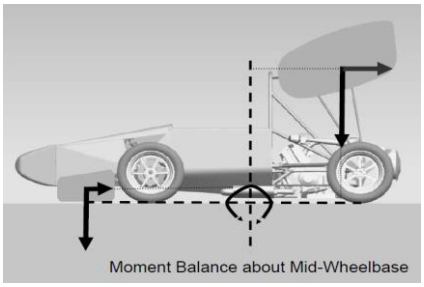

Figure 2 Balancing moments due to aerodynamic forces

Above calculations neglect drag forces on wings and forces due to undertray. The maximum allowable area for the front wing as per rule constraints is 0.525 m^2 [12]. All the calculations in this section were performed at 40 km/hr [6], which is the average speed of a car on track. The design values for front and rear wings are as follows,

$$C_{L,FW} = 2.93, C_{L,RW} = 3.6$$

The corresponding lap timing reduction for these design values is around 4 seconds.

As a concluding remark, the equation governing the motion of fluid around the car, Navier- Stokes is mentioned below.

$$\rho\left(\frac{\partial u_i}{\partial t} + u_j\frac{\partial u_i}{\partial x_j}\right) = -\frac{\partial p}{\partial x_i} + \mu\frac{\partial^2 u_i}{\partial x_j \partial x_j} + f_i \qquad (2)$$

where u is the velocity, t is the time, x is the position, p is the pressure and ρ is density.

PRELIMINARY DESIGN

With the design values established for front and rear wings, selection of airfoil was done based on literature review [3], [4], [5], [6], [7], [8] and [11]. As a huge library of airfoils was available at online database [15], the selection was made based on some key insights from the paper review.

- Thicker airfoils have larger C_{Lmax} (delayed stall)
- Increasing thickness (t/c), slightly increases the airfoil's lift curve slope
- Trailing edge of camber line has the largest effect on airfoil's lift
- For high lift, highly cambered airfoils should be used
- For low drag, less cambered and possibly thinner airfoils
- Data from racing industry reveals two types of airfoil usage: low drag & moderate lift or maximum lift

The design value of downforce coefficient for rear wing was very high, and difficult to achieve using a single airfoil wing. Hence, a multi-element wing was suitable for this application. For the main element, E 423 was used as it is widely used in motorsport competitions like Formula One, Indy Racing etc.; for flaps and slat S1223 airfoil is used as it is a high lift airfoil.

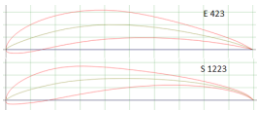

Figure 3 Airfoils E423 and S 1223

Front and Rear Wings

For 2D flow simulations over the airfoil sections, JAVAFOIL [16] was used as it is faster compared to any of the commercially available CFD packages like Fluent, OpenFoam etc. These simulations were useful for preliminary placement of airfoils. One notable limitation of this package is inviscid flow simulations (overestimation of downforce coefficient).

The first simulation was carried out using only the main element at an angle of attack of 10° as this value of the angle of attack is close to $C_{L,max}$ for the airfoil. Following the advice from Mcbeath [10], a four-element wing was explored, with 2 flaps, 1 slat, and 1 main element. Slat is 5% of the chord of main element and flaps are 15% of the chord of the main element in the following simulations. Various simulations were carried out to study the flow patterns and decide the relative location and orientation for the slat and flaps; this is more of a hit-and-trial process (Figure 4).

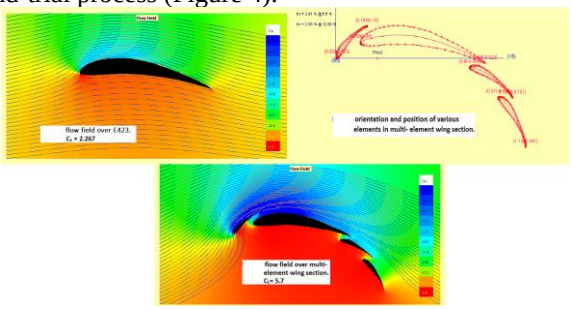

Figure 4 Flow field over rear wing elements

The value of downforce coefficient obtained for this configuration was 5.7, which was unreasonably large, as JAVAFOIL simulated an inviscid flow. This value was validated in ANSYS Fluent using a viscous laminar flow model to quantify the reduction in downforce due to friction (Fig. 5).

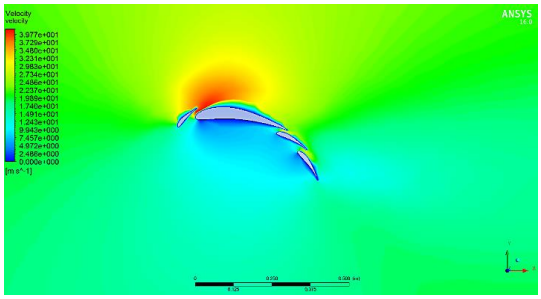

Figure 5 Velocity contour of rear wing elements in Fluent

Coupled scheme with PRESTO solver for pressure and second order upwind for momentum equations was used for these simulations. A value of 4.2 for downforce coefficient is obtained. A further reduction of value is to be expected due to finite wing span, which is around 0.2-0.3 [9]. This configuration was acceptable, as the value of downforce may further reduce due to other components on the car.

A similar approach was used for deciding front wing configuration. Downforce coefficient obtained from Fluent simulations was 3.6. For the front wing, downforce coefficient was overestimated by a larger value to account for additional rules [12], which effectively reduces the downforce produced by front wing. The CAD models for both wings are presented (Fig. 6). The front wing was modified to accommodate it around body works and as per the rule constraints [12].

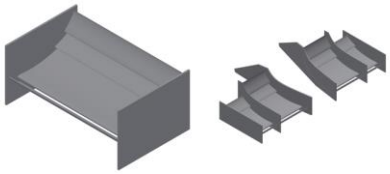

Figure 6 Rear (left) and front (right) wing CAD model

Undertray

Through white paper literature study, corroborated by the results of Jensen K [2], it was estimated that a rear diffuser only with a flat undertray can provide ~5-10 kgf of downforce at 18m/s. In order to verify this data, a reference diffuser was designed where the diffuser angles and lengths were dictated only by event regulations [12]. Simulations were carried out in Fluent with tire rotation and moving road conditions (Figure 7).

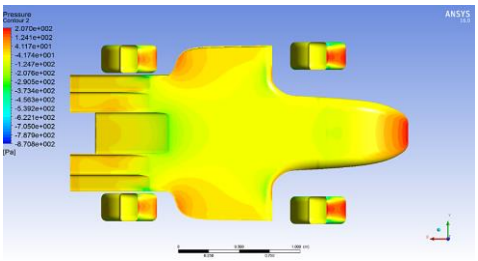

Figure 7 Pressure contour for undertray

A downforce of 6kgf was obtained, consistent with data from other similar designs reported by Jensen K [2]. The mass of an average FSAE car can be estimated to be about 250kg. The addition of ~6kg of downforce will only increase peak tire grip by ~2.5%, which will consequently increase cornering speed by only ~1.24%. This is not a significant performance gain. Therefore, a flat undertray is not ideal for FSAE applications. A contoured undertray was designed with channels of depth 15mm to further improve downforce produced by undertray (Figure 8).

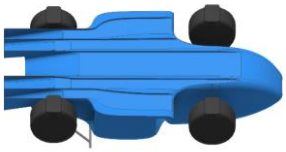

Figure 8 Contoured undertray with channels of depth 15mm

SIMULATIONS

In this section, 3D simulations performed in Fluent are discussed, along with results. Simulations of components are followed by full body simulations of the car.

The FSAE rules [12] constraint front and rear wings to be close to the ground, which induces the ground effect. Ground Effect changes the drag and downforce values of front wing substantially, as the ground clearance is a few millimeters.

Front Wings

Compared to the rear wing, the front wing is very close to the ground, which induces ground effect. This is caused primarily by the ground interrupting the wingtip vortices and downwash behind the wing.

Given below is the pressure contour for front wing close to the ground. For brevity, only comparative results (Table 1) are presented, for the case when front wings are far away from ground. The wing section has a span length of 600mm.

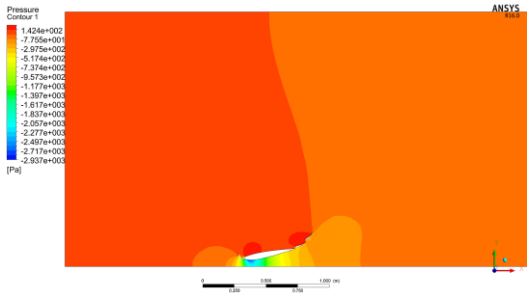

Figure 9 Pressure contour (2D section), wing close to ground

	Drag Force (N)	Downforce (N)
Without Ground Effect	5.28	76.07
With Ground Effect	13.09	139.03

Table 1 Comparative results of aerodynamic forces

As it can be observed from results (Table 1 and Fig. 9), both drag and downforce increase in the proximity of ground. This increase can be understood using continuity equation, which states: for an incompressible flow, as the cross-section area decreases, flow speed increases. The increase in flow speed causes a higher pressure gradient, which is reflected as an increase in drag and downforce. In this case, increase in the aerodynamic forces was approximately twice. Moreover, increase in downforce due to Ground Effect is useful as it helps in balancing the moment due to undertray, which was neglected in initial moment estimates.

Rear Wings

The airflow encountered by the front wing is cleaner compared to the rear wing, where main roll hoop causes turbulence (Figure 10). The effect of this turbulence on drag and downforce is studied in this subsection.

Figure 10 Main roll hoop

A wingspan of 600mm is used for simulations. The inlet turbulence is varied and corresponding values of drag and downforce are given below (Table 2).

Inlet Turbulence	Drag Force (N)	Downforce (N)
1%	5.3009	76.03
5%	5.302	76.10
20%	5.304	76.10

Table 2 Aerodynamic forces with varied inlet turbulence

As is observed from results, drag and downforce are almost constant. The aerodynamic forces are almost constant, as Z- component of circulation was absent in inlet turbulence boundary conditions. Further improvements due to Z-circulation were taken up in full body simulations.

Undertray

Contoured undertray (channels running along the length of undertray) provides significant benefits as it separates high-pressure air from the sides of the car from low pressure underneath it. For the first step of the iteration, the diffuser angle was varied to analyze the change in drag and downforce. As per FSAE regulations [12], vehicle's chassis, only the angle of the outermost diffuser can be varied. In order to speed up the iteration process, wheels were removed from these simulations in order to reduce computational cost (Figure 11).

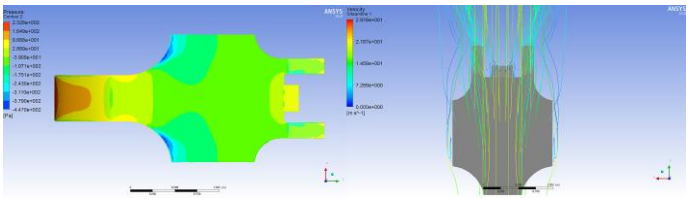

Figure 11 Contoured undertray simulations

Diffuser Angle, φ	C_D	C_L
12 °	0.4112	1.7241
18 °	0.4248	1.7889
24 °	0.4919	1.7902

Table 3 Variation in drag and downforce with diffuser angle

From the results, it can be concluded that the flow begins to separate between 18º and 24º. Hence, the diffuser angle is fixed at 18º to prevent flow separation and also, the increase in downforce coefficient with further increase in angle is negligible.

Full Body

The FSAE car is an open- wheel and open-cockpit, which introduces complexities in the flow field. Due to limited computation resources, a simplified model of car was used. The simplified car model consists of the complete aerodynamics package, body works, and a driver. Pressure contour (Figure 12) is presented for this simplified model. As can be observed, wheels have also been removed from these simulations and were accounted for in the benchmark studies later. Top- view of the model is presented in the figure below. The top part of the car is high-pressure region and stagnation point is located around the driver, marked by the red region.

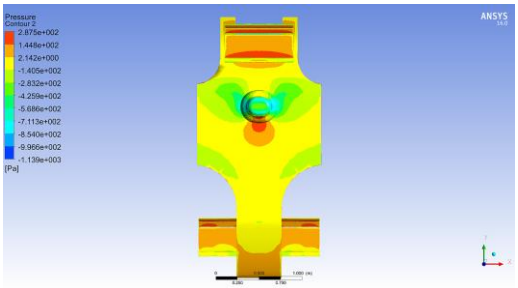

Figure 12 Pressure contour for simplified car model

The imbalance in moments due to increased downforce at front wing is studied by varying pitch angle of the car (Fig. 14).

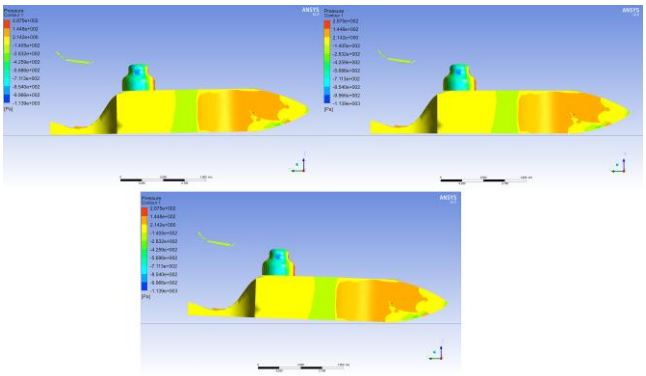

Figure 13 Pressure contours for variation of pitch angle

Here the sign convention for pitch angle is reversed as the direction of lift force (downforce) is also reversed. The results are presented below (Table 4).

Pitch Angle	Drag Force (N)	Downforce (N)
-2º	114.52	552.78
0º	103.93	589.12
2º	109.84	564.47

Table 4 Aerodynamic forces with variation in pitch angle

As can be observed from results (Fig. 13 and Table 4), drag increases and downforce decreases for non- zero pitch angle. This change in aerodynamic forces due to moment imbalance was corrected by making appropriate changes in the vehicle dynamics setup.

BENCHMARK STUDIES

Benchmark studies were conducted to select models for pressure and velocity, which helped in improving the overall estimate of downforce and drag coefficients for the car. The section starts with a benchmark study of Ahmed body and moves on to effects of tire squirt on the aerodynamic forces.

Ahmed Body

Complexly shaped cars are very challenging to model, which makes it difficult to quantify the aerodynamic forces computationally. The Ahmed body is a benchmark model widely used in the automotive industry for validating simulation tools. The Ahmed body shape is simple enough to model while maintaining car-like geometry features. The schemes used for simulations in the previous section were validated using this study. Originally described by S.R. Ahmed in 1984, the Ahmed body is widely used in the simulation of

external vehicle flows as a means of calibration. The schematic of Ahmed Body is presented in Figure 14.

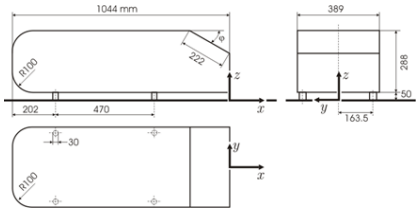

Figure 14 Ahmed body layout

For average operating speeds of a Formula SAE vehicle (15-20m/s), the Reynolds number is ~1.5x10^6. Using the experimental results of Ahmed [1], the coefficient of drag for this body at these Reynolds numbers was expected to be 0.33.

The above flow problem was then solved using a selection of turbulence models and discretization schemes. The error in the drag coefficient and the number of iterations to convergence were compared (Table 5).

Turbulence Model	Discretization	C_D	% error	Iterations to Convergence
Realizable k-epsilon, non-eq. wall function	Second order upwind for all variables	0.341753	3.56%	441
SST k-omega	Second order upwind for all variables	0.347121	5.19%	456
Realizable k-epsilon, non-eq. wall function	PRESTO for pressure, second order upwind for all other variables	0.336892	2.09%	378
SST k-omega	PRESTO for pressure, second order upwind for all other variables	0.340142	3.07%	382

Table 5 Results from Ahmed body simulations

Based on the simulations results, a realizable k-epsilon model with non- equilibrium wall functions and PRESTO schemes were selected for velocity and pressure discretization, respectively.

Effects of tire squirt on car

The tire is not only a major source of downforce but also causes significant turbulence in the lower parts of its wake. This turbulence, known as tire squirt in motorsport terminology, can severely affect the performance of ground effect devices like undertray. Flow around the car was simulated with and without wheels to understand the effects of tire squirt.

Results from simulations of the car with and without tires are presented in Table 6 and Figure 15.

	Without Wheels	With Wheels
Frontal Area	0.649m^2	0.726m^2
C_D	0.3956	0.5513
C_L	0.0426	0.2355

Table 6 Results from simulations with and without tires

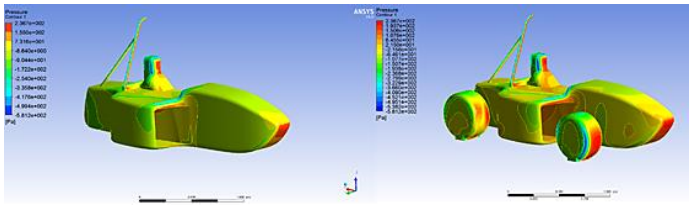

Figure 15 Pressure contours with and without tires

This study clearly proved that both drag and downforce coefficients are influenced by the presence of tires. Thus, helped in further improving the estimates of both drag and downforce. The effect of tire squirt is visible in the streamline pattern presented below (Figure 16).

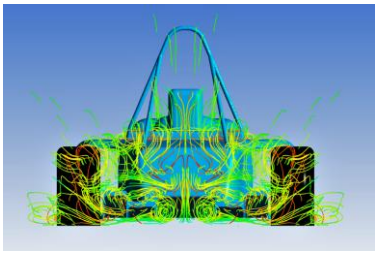

Figure 16 Flow separation behind car and tire squirt

OPTIMIZATION STUDY

For a specific configuration of a multi- element wing (number of elements in the wing), similar values for downforce can be obtained while reducing drag, by optimizing the relative placement of airfoil elements. This study aims to reduce drag on the car while achieving similar downforce values. Direct optimization available as a part of Optimization tools package [13] in ANSYS was used for this study. Direct optimization in ANSYS generates the design points and calculates the optimum solution depending on the output desired (Figure 17).

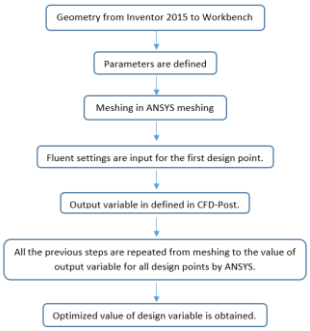

Figure 17 Direct optimization in ANSYS Workbench

For the first test case, discrete values of the parameters were supplied to the software; the vertical and horizontal distance between the two airfoils were used as parameters (Figure 18). The change in downforce coefficient with the decreasing horizontal distance (vertical distance kept constant) was studied.

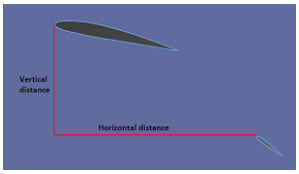

Figure 18 Airfoil arrangement for first test case

Coupled scheme with PRESTO solver for pressure and second order upwind for momentum equations. Results of this simulation were similar to experimental data available in Katz [9]: as horizontal distance between the two airfoils was reduced, lift coefficient increased.

Next, both the horizontal and the vertical distances were changed and their effect on the lift coefficient was studied. The horizontal distance has an upper limit of 200mm which has been selected from the studies in the previous case. Same geometry and settings for solver were used for this case. The results indicated that decrease in horizontal distance caused an increase in lift coefficient, and a decrease in vertical distance, increased lift coefficient up to a certain limit, beyond which the coefficient started decreasing again (Fig. 19). This can be understood by using the fundamental theorem of Aerodynamics: Kutta- Joukowski theorem, generally, which is used for calculation of lift of an airfoil in 2D. As the airfoils move closer, the sum of their respective circulations may be more or less, depending on the direction of circulation and their relative locations.

Table of Design Points

	A	B	C	D	E	F	G
1	Name	P1 - DS_horizontal	P2 - DS_vertical	P3 - lift	Retain	Retained Data	Note
2	Units			N			
3	DP 0 (Current)	0.2	0.4	232.58	☑	✓	
4	DP 1	0.15	0.4	234.1	☑	✓	
5	DP 2	0.1	0.4	233.16	☑	✓	
6	DP 3	0.05	0.4	230.38	☑	✓	
7	DP 4	0.04	0.4	228.67	☑	✓	
8	DP 5	0.03	0.4	243.24	☑	✓	
9	DP 6	0.02	0.4	238.5	☑	✓	
10	DP 7	0.01	0.4	245.31	☑	✓	
11	DP 8	0.005	0.4	227.49	☑	✓	
12	DP 9	0.2	0.3	239.8	☑	✓	
13	DP 10	0.2	0.2	244.59	☑	✓	
14	DP 11	0.2	0.1	248.37	☑	✓	
15	DP 12	0.2	0.05	232.9	☑	✓	
16	DP 13	0.2	0.04	235	☑	✓	
17	DP 14	0.2	0.03	228.91	☑	✓	
18	DP 15	0.2	0.02	224.14	☑	✓	
19	DP 16	0.2	0.01	222.64	☑	✓	
20	DP 17	0.2	0.005	225.68	☑	✓	
*					☐		

Figure 19 Results from the second case

This helped in understanding that relative location of airfoils in the multi-element wing play a crucial role in achieving high downforce coefficients. For the third case, an arrangement with 1 main element and 2 flaps was used (Fig. 20).

Figure 20 Airfoil arrangement for third test case

The objective here was to maximize the downforce coefficient; 100 design points were generated by Workbench and iterated to find the candidate points (Fig. 21).

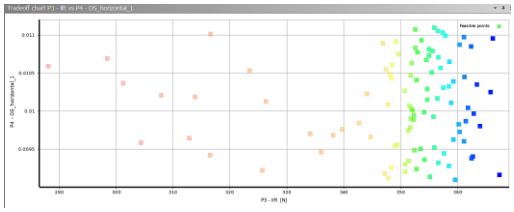

Figure 21 Trade-off chart of horizontal distance and downforce

Points on the right end of the chart represent high lift values; horizontal distance between airfoils is represented on the vertical axis. As can be observed in the chart, the lift force is increased with the addition of another flap to the second configuration.

Horizontal (mm)	Vertical (mm)	L (N)
9.16	26.522	367.42
10.959	23.88	366.2
10.252	25.813	365.85

Table 7 Candidate points from optimization study

These studies on direct optimization were important in understanding the usefulness of the optimization techniques available in ANSYS and help in evaluating the best possible configuration for various elements in wings before 3D simulations were performed.

CONCLUSION

An extensive aerodynamic study of a FSAE car was presented in this paper. Effects due to ground effect and turbulence were studied, which helped in refining the estimates of aerodynamic forces. Simulations of a contoured undertray and simplified full body model were also presented, which helped in assessing the design objectives. In the process of this study, benchmark studies and optimization studies were performed in ANSYS.

REFERENCES

[1] S.R. Ahmed, G. Ramm, and G. Faltin. Some salient features of the times-averaged ground vehicle wake. *SAE Society of Automotive Eng., Inc*, 1(840300):1–31, 1984.

[2] Karl Jensen, Aerodynamic Undertray Design for Formula SAE. *Masters of Science thesis, Oregon State University*

[3] Ponnappa Bheemaiah Meederira, Aerodynamic development of a IUPUI Formula SAE specification car with Computational Fluid Dynamics(CFD) analysis. *Masters of Science in Technology thesis, Purdue School of Engineering and Technology.*

[4] Marcello D.Guarro., Wing efficiency of race cars, *Ph.D. thesis, University of California, Santa Cruz.* May 2014

[5] James Patrick Merkel, Development of multi-element active aerodynamics for the Formula SAE car, *Masters of Science thesis, University of Texas-Arlington.* December 2013

[6] Wordley, S.J., and Saunders, J.W., Aerodynamics for Formula SAE: Initial Design and Performance Prediction, *SAE Paper* 2006-01-0806, 2006.

[7] Wordley, S.J., and Saunders, J.W., Aerodynamics for Formula SAE: A Numerical, Wind Tunnel and On-Track study, *SAE Paper* 2006-01-0808, 2006

[8] Angel Huminic and Gabriela Huminic, "On the Aerodynamics of the Racing Cars", 2008-01-0099.

[9] Katz, J., Race Car Aerodynamics: Designed for Speed, 2nd Edition, *Bentley Publisher*, ISBN 978-0-8376-0142-7.

[10] Simon McBeath, Competition Car Downforce: A Practical Guide, *Haynes Publications*, ISBN-13: 978-0854299775

[11] Pehan, S.and Kegl, B., Aerodynamics Aspects of Formula S Racing Car, *DS 30: Proceedings of DESIGN 2002, the 7th International Design Conference, Dubrovnik*, Pages: 1109-1118

[12] SAE, Formula Student Germany Rules 2016, December 2015

[13] ANSYS Inc., Documentation for Release 15.0

[14] OptimumG, OptimumLap Documentation

[15] http://www.airfoiltools.com

[16] Dr. Martin Hepperle, JAVAFOIL